Kinetics of conversion of celestite to strontium carbonate in solutions containing carbonate, bicarbonate and ammonium ions, and dissolved ammonia

MERT ZORAGA and CEM KAHRUMAN*

Istanbul University, Engineering Faculty, Metallurgical and Materials Engineering Department, 34320, Avcilar, Istanbul, Turkey

Abstract: Celestite concentrate ($SrSO_4$) was converted to $SrCO_3$ in solutions containing CO_3^{2-}, HCO_3^- and NH_4^+ and dissolved ammonia. The effects of stirring speed, CO_3^{2-} concentration; temperature and particle size of $SrSO_4$ on the reaction rate were investigated. It was found that the conversion of $SrSO_4$ was increased by increasing the temperature and decreasing the particle size, while the reaction rate was decreased with increasing the CO_3^{2-} concentration. However, the stirring speed had no effect on the reaction rate. The conversion reaction was under chemical reaction control and the shrinking core model was suitable to explain the reaction kinetics. The apparent activation energy for the conversion reaction was found to be 41.9 kJ mol^{-1}. The amounts of the elements in the reaction solution were determined quantitatively by inductively coupled plasma-optical emission spectrometry. The characterization of the solid reactant and product was made using the scanning electron microscopy-energy dispersive spectrometry and X-ray powder diffraction analytical techniques.

Keywords: celestite; strontium sulfate; strontium carbonate; conversion; kinetics.

INTRODUCTION

Celestite mineral is the main source of Sr metal and other Sr compounds. These are commonly used in a wide range of industrial applications, such as the production of ferrite magnets, pigments, special glasses, zinc refining and pyrotechnics, *etc*. The most important chemical compound of Sr is $SrCO_3$.

Typically, two methods are commonly used for the conversion of $SrSO_4$ to $SrCO_3$. In the first method (black ash method), $SrSO_4$ is reduced with coal in a furnace at temperatures between 1273 and 1473 K to produce soluble sulfide, which is then leached with water and the strontium-containing solution is reacted

---

* Corresponding author. E-mail: cemcemce@istanbul.edu.tr

345

with either CO_2 or Na_2CO_3 to precipitate $SrCO_3$.[1–3] However, this conventional process has high energy consumption and produces undesirable pollutants.[4,5] In the second method (direct conversion method), the conversion is maintained through the use of Na_2CO_3 or other carbonate sources.[2,3,6]

The conversion of $SrSO_4$ to $SrCO_3$ in alkali carbonate solution was studied by Kobe and Deiglmeir and it was found that 98.8 % conversion was obtained at 368 K after 2 h.[2] De Buda applied a two-staged purification process to obtain $SrCO_3$. Initially, HCl solution was used to extract impurities. Then, $(NH_4)_2CO_3$ solution was used to obtain $SrCO_3$.[7]

Kocakusak *et al.* used a $(NH_4)_2CO_3$ solution to convert $SrSO_4$ to $SrCO_3$. $SrCO_3$ was separated by filtration.[8] The filtrate consisted of $(NH_4)_2CO_3$ and $(NH_4)_2SO_4$. The $(NH_4)_2CO_3$ present in the solution was decomposed to NH_3 and CO_2 by heating the solution up to 353–373 K. The remaining solution was mixed with $Ca(OH)_2$ to precipitate $CaSO_4$. An ammoniacal solution was obtained by separating $CaSO_4$ by filtration. NH_3 and CO_2 obtained in the previous step was passed through this ammoniacal solution to obtain $(NH_4)_2CO_3$. This process has a significant economical importance in the industrial application of $(NH_4)_2CO_3$ solution as a reactant.

Erdemoglu and Canbazoglu[1] and Owusu and Litz[3] studied the leaching of SrS in water. Erdemoglu *et al.* investigated the leaching of celestite mineral in sodium Na_2S solution to obtain a Sr compound at constant temperature and determined the rate of conversion, which mainly depended on the Na_2S concentration. They concluded that the leaching of $SrSO_4$ in Na_2S solution was possible but slow.[9]

Aydogan *et al.* explained the dissolution kinetics of $SrSO_4$ in HCl solution containing $BaCl_2$ to produce $SrCl_2$. They claimed that the dissolution reaction of $SrSO_4$ was under chemical reaction control.[10]

Iwai and Toguri studied the conversion of $SrSO_4$ in Na_2CO_3 solution both from thermodynamic and kinetic points of view.[5] Castillejos *et al.* studied the conversion of $SrSO_4$ in Na_2CO_3 aqueous solution.[6] Erdemoglu *et al.*, Obut *et al.* and Setoudeh *et al.* investigated the direct mechano-chemical conversion of $SrSO_4$ to $SrCO_3$ using a ball mill.[11–13] Suarez-Orduna *et al.* and Ni *et al.* studied the conversion of $SrSO_4$ to $SrCO_3$ under hydrothermal conditions in Na_2CO_3 and hexamethylenetetramine solutions, respectively.[14,15] Bingöl *et al.* applied the neural model for the conversion of $SrSO_4$ in Na_2CO_3 solution and an extended delta–bar–delta algorithm.[16] In other studies by Bingöl *et al.*[17,18], the conversion of celestite with $(NH_4)_2CO_3$ to strontium carbonate were investigated using dry and wet mechano-chemical treatment in a planetary mill

The next step in the production of strontium metal are the calcinations of $SrCO_3$. These are typically performed by aluminothermic reduction followed by strontium evolution under vacuum.[19]

In this study, solutions containing CO_3^{2-}, HCO_3^- and NH_4^+ and dissolved NH_3 were used to determine the effects of stirring speed, particle size of $SrSO_4$, CO_3^{2-} concentration and temperature on the conversion of high-grade celestite mineral to $SrCO_3$. A kinetic model equation was derived, which showed the relationship between the fractional conversion of $SrSO_4$ (X) with time (t) and particle size (R).

EXPERIMENTAL

Celestite concentrate

The celestite concentrate used in this study was provided by Barit Maden Turk A.S., Turkey. The quantitative chemical composition of the celestite concentrate, determined by X-ray fluorescence spectroscopy (XRF) analysis, is given in Table I. The mineral consisted of 96.79 mass % $SrSO_4$. The celestite concentrate was subjected to particle size distribution using the standard test sieves by the wet sieve equipment Octagon 200.

TABLE I. Composition of celestite concentrate

Compound	$SrSO_4$	$CaSO_4$	$BaSO_4$	SiO_2	Fe_2O_3
Content, mass %	96.79	2.04	0.57	0.46	0.14

Preparation of the solution containing CO_3^{2-}, HCO_3^-, NH_4^+ and dissolved NH_3

The commercially available $(NH_4)_2CO_3$ was in the form of a mixture of ammonium carbamate ($H_4NOCONH_2$) and ammonium bicarbonate ($H_4NOCOOH$) in a mole ratio of 1:1 (Merck, 1.59504.1000) (AC). Different amounts of this substance were dissolved in distilled water to obtain solutions that contained CO_3^{2-}, HCO_3^{-1}, NH_4^+ and dissolved NH_3, which were used in the conversion reactions.

Volumetric analysis

The concentrations of CO_3^{2-}, HCO_3^- and of NH_3 dissolved in the solutions were determined quantitatively by volumetric analyses by titrating with a definite volume of solution of HCl titrisol solution (Merck), using first phenolphthalein and then methyl orange as the indicator.

Experimental procedure

The experiments were performed using the set-up illustrated in Fig. 1-S of the Supplementary material to this paper. A detailed explanation of the employed set-up was described by Kalpakli et al.[20] For the determination of the amounts of the elements dissolved in the solution, a definite volume of solution was taken from the reactor at definite time intervals during the reaction. The same amount of fresh AC solution was added to the reactor after each sampling. In this way, the concentrations of CO_3^{2-}, HCO_3^{-1}, NH_4^+ and dissolved NH_3 and the total volume of the reaction mixture were kept constant during the experiments. The quantitative analysis of the elements in the solution was realized using inductively coupled plasma-optical emission spectrometry (ICP-OES, Spectro Ciros Vision).

Materials characterization

For the characterization of the solid reactant (celestite concentrate, $SrSO_4$) and solid product ($SrCO_3$) obtained at the end of each experiment, X-ray powder diffraction analysis (XRD, Rigaku D/Max-2200/PC, CuK$_\alpha$ (1.54056 Å) and scanning electron microscopy–energy

dispersive spectroscopy (SEM–EDS, Jeol JSM 5600- i-XRF 500i) analytical techniques were used.

RESULTS AND DISCUSSION

The dissolution of AC in pure water

During the dissolution of AC in pure water, dissolution (Reaction (1)) and hydrolysis (Reaction (2)) reactions occur simultaneously:

$$H_4NOCOOH(s) \rightarrow HCO_3^-(aq) + NH_4^+(aq) \tag{1}$$

$$H_4NOCONH_2(s) \rightarrow CO_3^{2-}(aq) + 2\,NH_4^+(aq) \tag{2}$$
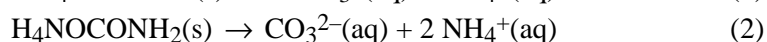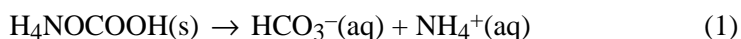
The HCO_3^- and NH_4^+ that were formed according to Reactions (1) and (2) are hydrolyzed rapidly as shown in Reactions (3) and (4). For simplicity, H_3O^+ is written as H^+:

$$NH_4^+(aq) \rightleftarrows NH_3(l) + H^+(aq) \tag{3}$$

$$HCO_3^-(aq) \rightleftarrows CO_3^{2-}(aq) + H^+(aq) \tag{4}$$
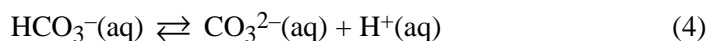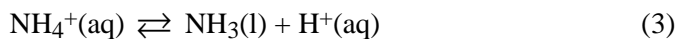
The H^+ that are formed in Reaction (3) are consumed by CO_3^{2-} in the reverse Reaction (4), and thus the equilibrium reaction (Reaction (5)) is effective:

$$CO_3^{2-}(aq) + NH_4^+(aq) \rightleftarrows NH_3(l) + HCO_3^-(aq) \tag{5}$$
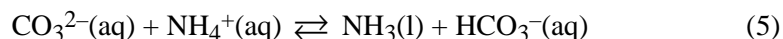
The dependency of the acid dissociation constants (K_3 and K_4) of Reactions (3) and (4) with temperature are given by Eqs. (6) and (7).[21,22] In these equations, T is the absolute temperature and pK is defined as $-\log K$.

$$pK_3 = 0.090387 + 2729.33/T \tag{6}$$

$$pK_4 = -6.4980 + 2902.39/T + 0.02379 \tag{7}$$

The equilibrium constant of Reaction (5), K_5, was calculated using Eqs. (6) and (7) for each solution temperature applied in the experiments. The calculated values of K_5 are given in Table II. These values were used to calculate CO_3^{2-}, HCO_3^- and NH_4^+ concentrations and the molecularly dissolved NH_3 concentrations for different amounts of AC and temperature (Table III). Table III shows that at constant temperature, as the AC quantity increased, the ion concentrations in the solution increased. When the AC quantity was kept constant, the CO_3^{2-} and NH_4^+ concentrations decreased, while the molecularly dissolved NH_3 and HCO_3^- concentration increased with increasing temperature. The heat of equilibrium reaction (Reaction (5)) was calculated to be positive (endothermic reaction) by using Gibbs–Helmholtz Equation and Eqs. (6) and (7).[23] The enthalpy change of Reaction (5) were found to be 35.8, 38.5, 41.3 and 44.2 kJ mol^{-1} for 293, 303, 323 and 323 K, respectively. Since Reaction (5) was calculated to be endothermic, the reaction proceeded towards the right hand side. Thus, the CO_3^{2-} and NH_4^+ concentrations decreased with increasing temperature of the solution.

TABLE II. Equilibrium constants for Reaction (5) at different temperatures

T / K	293	303	313	323
K_5	9.391	15.529	25.751	42.813

TABLE III. Concentrations of CO_3^{2-}, HCO_3^-, NH_4^+ and NH_3 dissolved in AC aqueous solutions

T / K	AC concentration, mol dm^{-3}				
	0.5	0.75	1.00	1.25	1.50
Concentration of CO_3^2, mol m^{-3}					
293	44	65	89	111	133
303	29	43	57	72	86
313	18	27	36	45	55
323	11	17	22	28	33
Concentration of HCO_3^-, mol m^{-3}					
293	956	1435	1911	2389	2867
303	971	1457	1943	2428	2914
313	982	1473	1964	2455	2946
323	989	1483	1978	2472	2967
Concentration of dissolved NH_3, mol m^{-3}					
293	456	685	911	1139	1367
303	471	707	943	1178	1414
313	482	723	964	1205	1446
323	489	733	978	1222	1467
Concentration of NH_4^+, mol m^{-3}					
293	1044	1565	2089	2611	3133
303	1029	1543	2057	2572	3086
313	1018	1527	2036	2545	3055
323	1011	1517	2022	2528	3033

H^+ and OH^- exist in the solution together with CO_3^{2-}, HCO_3^-, NH_4^+ and molecularly dissolved NH_3. Consequently, these determine the pH of the solution. It is important to note that H^+ and OH^- concentrations were quite low with respect to the concentrations of the other ion.

The concentration values given in Table III are in good agreement with the results of volumetric analyses. The consumption of HCl titrisol solution for the change in the color of the phenolphthalein indicator was determined to be half that consumed for a change of the color of the Methyl Orange indicator. During the titration with HCl titrisol solution using the phenolphthalein indicator, CO_3^{2-} and NH_3 present in the solution are transformed to HCO_3^- and to NH_4^+, respectively. In the following step, after the addition of the methyl orange indicator, the HCO_3^- formed in the first step and the HCO_3^- already present in the solution were titrated to from H_2CO_3, which leaves the solution as CO_2 gas.

The pH values of the solutions were measured to be 8.9 at room temperature (298 K) in all the solutions obtained by dissolving different amounts of AC. The

mole ratios of HCO_3^- to CO_3^{2-} and NH_4^+ to NH_3 in each solution were constant for each temperature. The pH value of the solution was also calculated according to Eqs. (6) and (7) to be 8.9 again. The same calculated and measured pH values of the solution suggest that the activity coefficients of each reactant and product, which are dependent to the ionic strength of the solution, did not change the value of K_5.

The equilibrium between ammonium carbonate, ammonium bicarbonate and ammonium carbamate was investigated with Raman spectroscopy by Wen and Broker.[24] They claimed that carbamate ions (H_2NCOO^-) existed in the solution together with CO_3^{2-}, HCO_3^-, NH_3 and NH_4^+. Qin *et al.* observed that H_2NCOO^- is present in the aqueous solutions of NH_3 containing ammonium carbonate/ /ammonium bicarbonate.[25] Therefore, in this study, the prepared AC solution was held for a long period in a closed flask for the complete hydrolysis of H_2NCOO^-. The measured pH was found to be the same as the calculated one, which indicates that complete hydrolysis was achieved.

The conversion of SrSO$_4$ to SrCO$_3$

The driving force for the conversion reaction if $SrSO_4$ to $SrCO_3$ is the low solubility of $SrCO_3$ compared to $SrSO_4$ in aqueous solutions. The solubility products of $SrSO_4$ and $SrCO_3$ are 2.8×10^{-7} and 9.4×10^{-10}, respectively.[11] Thus, the solubilities of $SrSO_4$ and $SrCO_3$ in pure water were calculated to be 0.529 and 3.07×10^{-2} mol m^{-3}, respectively.

The conversion of $SrSO_4$ to $SrCO_3$ in the solutions containing CO_3^{2-}, HCO_3^-, NH_4^+ and dissolved NH_3 occurs according to:

$$SrSO_4 + CO_3^{2-} \rightarrow SrCO_3 + SO_4^{2-} \qquad (8)$$
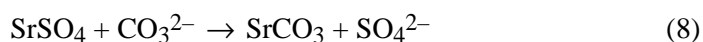
The concentration of CO_3^{2-} in the solution did not change significantly during the conversion due to the use of small amounts of celestite (0.016 mol) with respect to large concentrations of NH_3 and HCO_3^- present in the used solution. This is due to fact that during the consumption of CO_3^{2-} according to Reaction (8), CO_3^{2-} are simultaneously rapidly formed according to reverse Reaction (5). Therefore, the concentration of CO_3^{2-} did not change during the conversion reaction, which is of importance in terms of the kinetic evaluation.

The effect of stirring speed

A celestite concentrate of 0.016 mol (53–75 µm particle size, 1×10^{-3} m^3 solution, 1.5 mol of AC and 323 K) was used at 3.33, 4.17 and 5 rps to investigate the effect of stirring speed on the conversion reaction of $SrSO_4$.

The fractional conversion of $SrSO_4$ (X) at any reaction time (t) was calculated according to:

$$X = \frac{W_0 - W_t}{W_0} \qquad (9)$$

where W_0 is the mass of $SrSO_4$ fed to the solution and W_t is the mass of unreacted $SrSO_4$ at any reaction time, t.

The X–t diagrams obtained for 3.33, 4.17 and 5 rps are illustrated in Fig. 2, from which it can be seen that increasing the stirring speed from 3.33 to 5 rps had no significant effect on the reaction rate. This case proved that the use of 5 rps. can eliminate the resistance of the liquid film surrounding the particles. Therefore, in the experiments in which the effects of the other parameters on the conversion were investigated, the stirring speed was kept constant at 5 rps.
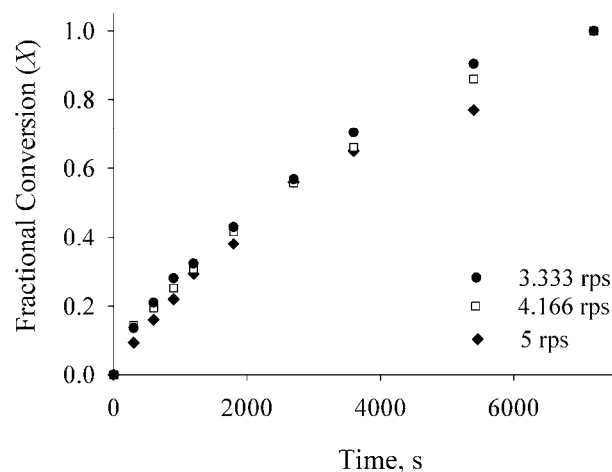

Fig. 2. The effect of stirring speed on the fractional conversion of $SrSO_4$ (temperature: 323 K, CO_3^{2-} concentration: 33 mol m^{-3} and particle size: 53– –75 μm).

The effects of temperature and CO_3^{2-} ion concentration

The experiments were not performed at temperatures above 323 K, since the AC solution decomposed at 331 K. Celestite concentrate (0.016 mol) with particle sizes of 53–75μm, a 1×10^{-3} m^3 solution of AC that was obtained by dissolving 0.5, 0.75, 1, 1.25 or 1.5 mol of AC were investigated at 293, 303, 313 of 323 K to study the effects of temperature and CO_3^{2-} concentration on the conversion reaction of $SrSO_4$. The concentrations of CO_3^{2-}, HCO_3^-, NH_4^+ and molecularly dissolved NH_3 used in the experiments are given in Table III. It can be clearly seen that with increasing AC, all of the concentrations (CO_3^{2-}, HCO_3^-, NH_4^+ and molecularly dissolved NH_3) increased. On the other hand, with increasing temperature, the CO_3^{2-} and NH_4^+ concentrations decreased while the concentrations of HCO_3^- and molecularly dissolved NH_3 increased. The typical X vs. t diagrams at different temperatures and CO_3^{2-} concentrations are shown in Fig. 3 (other investigated cases are shown in Fig. 2-S of the Supplementary material), from which it could be seen that for each constant temperature, the frac-

tional conversion decreased with increasing concentration of CO_3^{2-}, which indicates that the conversion rate is inversely proportional to the CO_3^{2-} concentration. Although the CO_3^{2-} concentration is lower, X increased with increasing temperature, which is in accordance with the Arrhenius Equation, as expected.
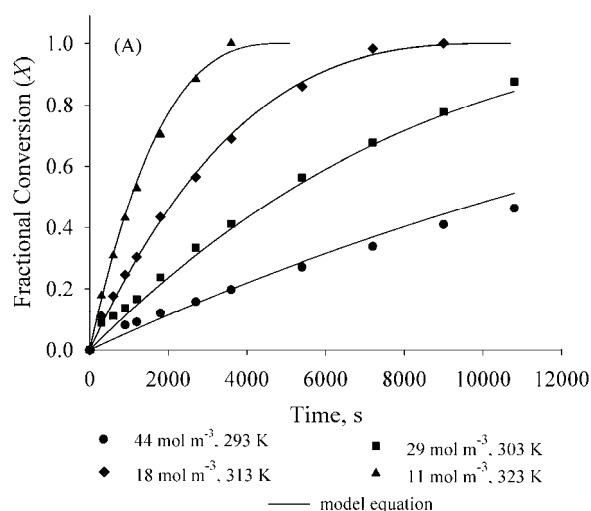

Fig. 3. The effects of temperature and CO_3^{2-} concentration on the fractional conversion of SrSO$_4$ (particle size: 53–75 μm, stirring speed: 5 rps).

The effect of particle size

For the determination of the effect of particle size on the conversion of SrSO$_4$, 90–125, 53–75 and 38–45 μm sized particles were used. The experimental conditions were 0.016 mol celestite concentrate, 1×10^{-3} m^3 solution that was obtained by dissolving 1 mol AC, 323 K and 5 rps. The X *vs. t* diagrams are shown in Fig. 4. It was observed that the fractional conversion of SrSO$_4$ increased with decreasing particle size.

Materials characterization

The XRD and SEM–EDS analytical techniques were applied to characterize the celestite concentrate and the solid product obtained during the conversion reaction using 0.016 mol of celestite concentrate with a particle size of 53–75 μm, 1×10^{-3} m^3 solution, 0.5 mol of AC, 323 K and 5 rps. The XRD patterns and SEM–EDS images of the celestite concentrate and solid product are presented in Figs. 5 and 6, respectively, from which it can be seen that the celestite concentrate contained mainly SrSO$_4$ and the reaction product SrCO$_3$.
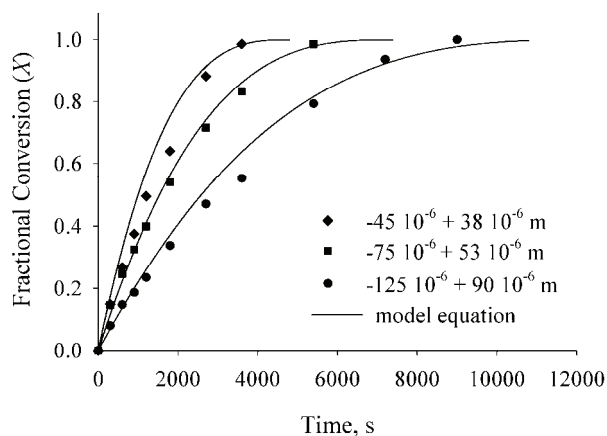
Fig. 4. The effect of particle size on the fractional conversion of $SrSO_4$ (temperature: 323 K, CO_3^{2-} concentration: 22 mol m^{-3}, stirring speed: 5 r.p.s.)
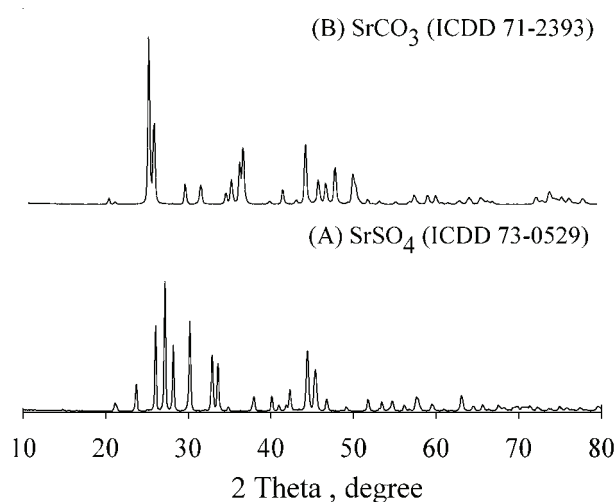

Fig. 5. XRD diagrams, A – celestite concentrate ($SrSO_4$) and B – reaction product ($SrCO_3$).

Kinetic evaluation of conversion reaction

The molar volumes of $SrSO_4$ and $SrCO_3$ are 46.38×10^{-6} and 39.47×10^{-6} m^3 mol^{-1}, respectively. The lower molar volume of $SrCO_3$ is an indication that the product layer that surrounds the reactant had to be porous. In order for the reaction to proceed, CO_3^{2-} have to diffuse through the pores of the $SrCO_3$ layer towards the surface of $SrSO_4$ and the SO_4^{2-} that are formed during the conversion reaction have to diffuse through the same porous layer in the opposite direction towards the solution. When the resistance of the pores of the product layer is high, the reaction becomes diffusion controlled. If the sizes of the pores of the product layer are large enough, the reaction will be chemically controlled.

According to the "shrinking core model",[26] in the case of the establishment of a constant temperature (isothermal condition) and a constant CO_3^{2-} concen-

tration on the surface of the dense spherical particles of SrSO$_4$, if the reaction is under chemical reaction control, the change of X with t is given by:

$$1-(1-X)^{1/3} = \frac{bkc^m}{\rho r}t = \lambda t \qquad (10)$$

where b denotes the stoichiometric coefficient, k the reaction rate constant, c the CO$_3^{2-}$ concentration, m the reaction order for CO$_3^{2-}$, ρ the density of the SrSO$_4$ particles and r the average radius of the particles. When $1-(1-X)^{1/3}$ *vs*. t diagrams are plotted, the slope of these straight lines gives λ. It can be seen in Fig. 7 (some additional examples are given in Fig. 3-S of the Supplementary material) that the relationship between $1-(1-X)^{1/3}$ and t was linear. This finding shows that the topochemical reaction was under chemical control.

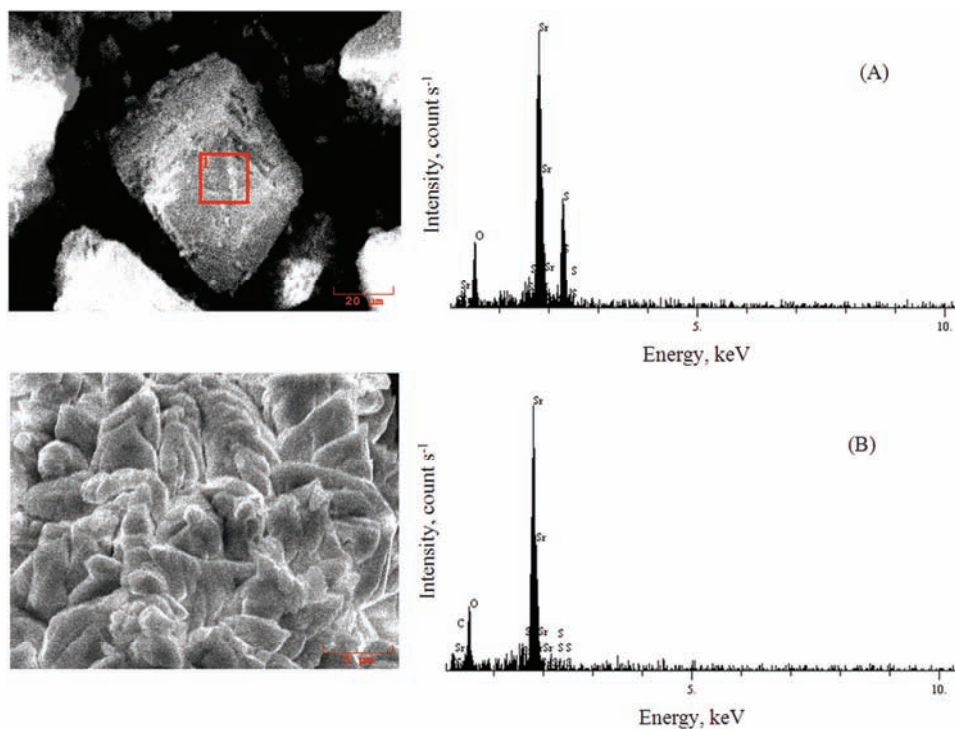Fig. 6. SEM images and EDS analyses, A – celestite concentrate and B – reaction product.

Considering Eq. (10), at constant temperature and various CO$_3^{2-}$ concentrations, Eq. (11) is valid:

$$\lambda = \alpha c^m \qquad (11)$$

where α is given by $bk / \rho R$. The natural logarithm of Eq. (11) gives Eq. (12):

$$\ln \lambda = \ln \alpha + m \ln c \tag{12}$$

According to Eq. (12), the slope of $\ln \lambda$ *vs.* $\ln c$ will give m. The intersection at the ordinate axis gives $\ln \alpha$ when $\ln c \to 0$. The term α in Eq. (12) includes k. For various CO_3^{2-} concentrations at constant temperatures, $\ln \lambda$ *vs.* $\ln c$ diagrams are plotted in Fig. 8, from which it can be seen that parallel straight lines with slopes of $-1/2$ were obtained, which is the value of m. The k values were calculated from the α values by considering that $r = 64 \times 10^{-6} m$, $\rho = 21600$ mol m^{-3} and $b = 1$. The change of k with the absolute temperature can be determined by the Arrhenius Equation (Eq. (13)):

$$\ln k = \ln A_0 - \frac{E_a}{RT} \tag{13}$$

where A_0 is the pre-exponential factor, E_a the apparent activation energy and R the gas constant.
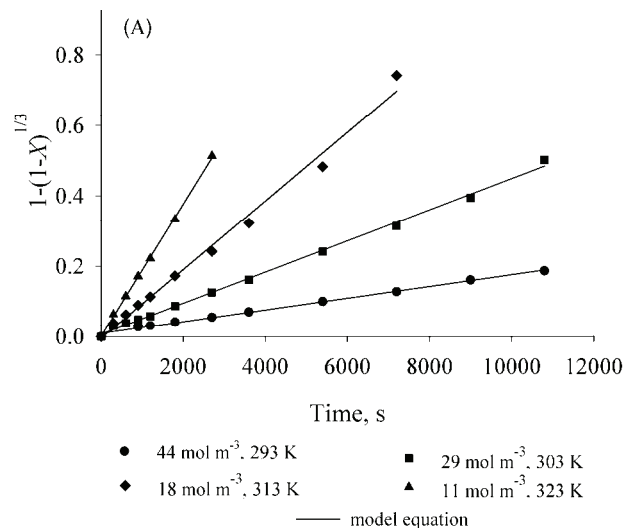

Fig. 7. $1-(1-X)^{1/3}$ *vs.* time diagrams for different concentrations of CO_3^{2-} and temperatures.

The relationship between $\ln k$ and $1/T$ is shown in Fig. 9. The slope of this line gives $-E_a/R$ and intercept at the ordinate axis for $1/T = 0$ gives $\ln A_0$. From these values, E_a was calculated as 41.9 kJ mol^{-1} and A_0 as 171.2 (mol m^{-3})$^{3/2}$ m s^{-1}.

Equation (14) was obtained by replacing the ρ and b values with the calculated values of A_0, E_a and m in Eq. (10):

$$X = 1 - \left[1 - \frac{171.2 e^{-5046.22/T}}{21600 r} c^{-1/2} t \right]^3 \tag{14}$$

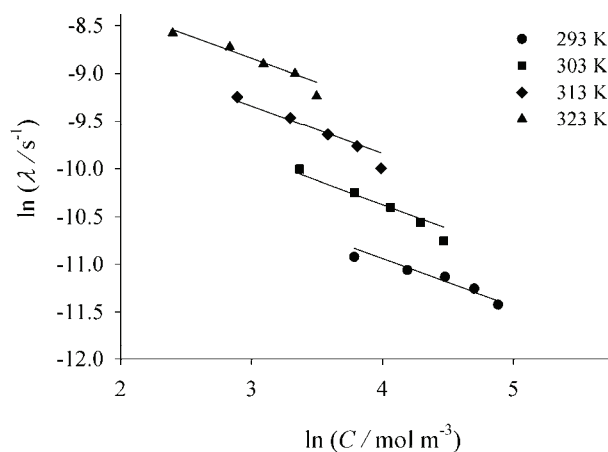Equation (14) shows the change of *X* with respect to *R* and *t*.

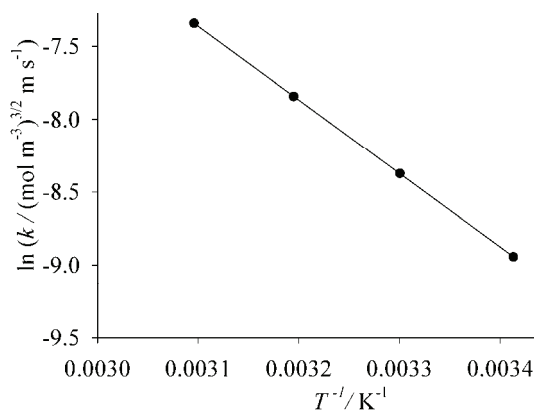Fig. 8. ln λ *vs.* ln *c* diagrams.

Fig. 9. Arrhenius plot (ln *k* *vs.* *T*⁻¹ diagram).

All of the continuous lines given in Fig. 3 represent *X vs. t*, which were calculated and drawn according to Eq. (14). As can be seen in Fig. 3, there is a good agreement between the experimentally obtained values and the diagrams drawn using Eq. (14). Moreover, the *X vs. t* diagrams drawn using Eq. (14) for the different investigated particle sizes are shown as continuous lines in Fig. 4. Again, there is a good agreement between the experimental values and the diagrams plotted according to Eq. (14) using different *r* values.

Iwai and Toguri studied the conversion of celestite in Na_2CO_3 solution and concluded that during the initial stage of the reaction, the conversion rate was controlled by the dissolution rate of $SrSO_4$ and, therefore, the reaction rate was independent of the concentration of CO_3^{2-} (zero order).[5] They indicated that as the reaction proceeds, a $SrCO_3$ layer will be densely deposited on the celestite surface. As a result, the rate-determining step changed to the diffusion rate of

SO_4^{2-} through the pores of $SrCO_3$. They concluded that the decrease in the conversion with increasing CO_3^{2-} concentration was a result of the change in the morphology of the $SrCO_3$. They obtained apparent activation energies of 71.5 and 64.1 kJ mol^{-1} for the surface reaction and the diffusion step, respectively.

Castillejos *et al.* investigated the effects of stirring speed, particle size, Na_2CO_3 and Na_2SO_4 concentrations, temperature, solution pH and solid/liquid ratio on the conversion reaction of $SrSO_4$ to $SrCO_3$ in solutions containing Na_2CO_3.[6] They concluded that the reaction is topochemical, and the rate-determining step is the diffusion rate of CO_3^{2-} through the pores of the product layer. They found that the reaction rate increased with increasing temperature and decreasing particle size. They calculated an apparent activation energy for the diffusion rate of 70.0 kJ mol^{-1}.

The activation energy reported by Iwai *et al.* of 64.1 kJ mol^{-1} is in agreement with that reported by Castillejos *et al.* (70.0 mol^{-1}).[5,6] It is unlikely that reactions under diffusion rate control would have a high value of the activation energy. Thus, Castillejos *et al.* concluded that the high value of the activation energy for the reaction under diffusion rate control is indicative of the production of a compact layer with very tortuous pores. Therefore, the effective diffusivities calculated in their work fell in the range between 1.2×10^{-13} and 6.7×10^{-12} m^2 s^{-1}.[6]

The findings of Bingol *et al.* were similar to those of Iwai and Toguri and Castillejos *et al.* [5,6,16] They claimed that the conversion reaction was nearly completed at 333 K within 4 h and a neural model was used for computing the conversion kinetics.

In the above-mentioned studies, the pH of the solution was high (11–12). However, in the present study, the reaction proceeded at lower pH (8.22–9.04) and CO_3^{2-} concentrations 11–133 mol m^{-3} because of the rapid equilibrium reaction (Reaction (5)) with respect to conversion reaction (Reaction (8)). In this study, it was determined that the reaction rate was under chemical reaction rate control and the activation energy for the reaction was calculated to be 41.9 kJ mol^{-1}. The reaction rate was found to be inversely proportional to the CO_3^{2-} concentration. It was found that the kinetic model equation (Eq. (14)) derived in this study was in good agreement with all the experimentally obtained fractional conversion values at different reaction times.

CONCLUSIONS

The complete dissolution of ammonium bicarbonate and hydrolysis of ammonium carbamate present in AC gave a aqueous solution that contained CO_3^{2-}, HCO_3^-, NH_4^+ and dissolved NH_3.

During the conversion of $SrSO_4$, porous $SrCO_3$ formed on the surfaces of the $SrSO_4$ particles, enabling the total conversion of $SrSO_4$.

A stirring speed of 5 rps was sufficient to eliminate the resistance of the liquid film that surrounds the surfaces of the $SrSO_4$ particles.

The conversion rate increased with increasing temperature and decreasing particle size, whereas it decreased with increasing CO_3^{2-} concentration.

The heterogeneous reaction kinetics of solid $SrSO_4$ particles with CO_3^{2-} in aqueous solution was explained with the "shrinking core model". The topochemical reaction was under chemical reaction control. The reaction order for CO_3^{2-}, the activation energy and the pre-exponential factor were calculated to be $-1/2$, 41.9 kJ mol^{-1} and 171.23 (mol m^{-3})$^{3/2}$ m s^{-1}, respectively. The derived kinetic model equation was in good agreement with all the experimental conversion values obtained at different reaction times.

SUPPLEMENTARY MATERIAL

Experimental set up, X and $1-(1-X)^{1/3}$ *vs.* time diagrams are available electronically from http://www.shd.org.rs/JSCS/, or from the corresponding author on request.

ИЗВОД

КИНЕТИКА КОНВЕРЗИЈЕ ЦЕЛЕСТИТА У СТРОНЦИЈУМ-КАРБОНАТ У РАСТВОРИМА КАРБОНАТНИХ, БИКАРБОНАТНИХ, АМОНИЈУМ ЈОНА И АМОНИЈАКА

MERT ZORAGA и CEM KAHRUMAN

Istanbul University, Engineering Faculty, Metallurgical and Materials Engineering Department, 34320, Avcilar, Istanbul, Turkey

Концентрат целестита ($SrSO_4$) конвертован је у $SrCO_3$ у растворима који су садржали CO_3^{2-}, HCO_3^-, NH_4^+ и растворени амонијак. Испитивани су ефекти брзине мешања, концентрације CO_3^{2-}, температуре и величине честица $SrSO_4$ на брзину реакције. Утврђено је да брзина конверзије $SrSO_4$ расте са температуром и смањивањем величине честица, а опада са повећањем концентрације CO_3^{2-}. Конверзију контролише хемијска реакција, а за објашњење кинетике реакције показао се погодним „*shrinking core model*". Одређена је вредност енергије активације реакције конверзије од 41,9 kJ mol^{-1}. Састав реакционог раствора одређиван је куплованом методом плазма − оптичка емисиона спектроскопија. Чврсти реактанати и производи окарактерисани су скенирајућом електронском микроскопијом са енергетском дисперзионом спектроскопијом (SEM−EDS) и техником ренгенске дифракције праха (XRD).

(Примљено 7. марта, ревидирано 21. маја 2013)

REFERENCES

1. M. Erdemoglu, M. Canbazoglu, *Hydrometallurgy* **49** (1998) 135
2. K. A. Kobe, N. J. Deiglmeier, *Ind. Eng. Chem.* **35** (1943) 323
3. G. Owusu, J. E. Litz, *Hydrometallurgy* **57** (2000) 23
4. H. Dogan, M. Koral, S. Kocakusak, *Hydrometallurgy* **71** (2004) 379
5. M. Iwai, J. M. Toguri, *Hydrometallurgy* **22** (1989) 87

6. A. H. Castillejos-Escobar, F. P. De La Cruz-Del Bosque, A. Uribe-Salas, *Hydrometallurgy* **40** (1996) 207
7. F. De Buda, U.S. Patent 4,666,688 (1987)
8. S. Kocakusak, R. Tolun, H. Dogan, K. Akcay, H. J. Koroglu, H. Yuzer, M. Koral, F. Isbilir, O. T. Savascı, T. Ayok, Patent No: TR2001/0326521.5 (2003)
9. M. Erdemoglu, M. Sarıkaya, M. Canbazoglu, *J. Dispers. Sci. Technol.* **27** (2006) 439
10. S. Aydogan, M. Erdemoglu, A. Aras, G. Ucar, A. Ozkan, *Hydrometallurgy* **84** (2006) 239
11. M. Erdemoglu, S. Aydogan, M. Canbazoglu, *Hydrometallurgy* **86** (2007) 1
12. A. Obut, P. Balaz, I. Girgin, *Miner. Eng.* **19** (2006) 1185
13. N. Setoudeh, N. J. Welham, S. M. Azami, *J. Alloy. Compd.* **492** (2010) 389
14. R. Suarez-Orduna, J. C. Rendon-Angeles, K. Yanagisawa, *Int. J. Miner. Process.* **83** (2007) 12
15. S. Ni, X. Yang, T. Li, *Mater. Lett.* **65** (2011) 766
16. D. Bingol, S. Aydogan, S. S. Gultekin, *Chem. Eng. J.* **165** (2010) 617
17. D. Bingöl, S. Aydogan, S. K. Bozbas, *J. Ind. Eng. Chem*. **18** (2012) 834
18. D. Bingöl, S. Aydogan, S. K. Bozbas, *Metall. Trans., B* **43** (2012) 1214
19. F. Habashi, *Handbook of Extractive Metallurgy (Vol.4 Ferroalloys Metals, Alkali Metals, Alkaline Earth Metals)*, Wiley–VCH, Weinheim, 1997, p. 2333
20. A. O. Kalpakli, S. Ilhan, C. Kahruman, I. Yusufoglu, *Hydrometallurgy* **121**–**124** (2012) 7
21. W. J. Cai, Y. Wang, *Oceanography* **43** (1998) 657
22. S. Clegg, M. Whitfield, *Geochim. Cosmochim. Acta* **59** (1995) 122403
23. D. R. Gaskell,. *Introduction to the Thermodynamics of Materials,* 4th ed., Taylor & Francis, New York, 2003, p. 102
24. N. Wen, M. H. Brooker, *J. Phys. Chem*. **99** (1995) 359
25. F. Qin, S. Wang, I. Kim, H. F. Svendsen, C. Chen, *Int. J. Greenh. Gas Con.* **5** (2011) 405
26. O. Levenspiel, *Chemical Reaction Engineering*. 3rd ed., Wiley, New York, 1999, p. 575.